Potential-driven on/off switch strategy for the electrosynthesis of [7]helicene-derived polymers

Jan Hrbáč,[a] Tomáš Strašák,[b] Ladislav Fekete,[c] Vít Ladányi,[a] Jan Pokorný,[c] Jiří Bulíř,[c] Miloš Krbal,[d] Jaroslav Žádný,[b] Jan Storch,[b],* and Jan Vacek[e],**

[a] Institute of Chemistry, Masaryk University, Kamenice 5, 725 00 Brno, Czech Republic

[b] Institute of Chemical Process Fundamentals, Czech Academy of Sciences, Rozvojova 135, 165 02 Prague 6, Czech Republic

[c] Institute of Physics, Czech Academy of Sciences, Na Slovance 2, Prague, Czech Republic

[d] Center of Materials and Nanotechnologies (CEMNAT), Faculty of Chemical Technology, University of Pardubice, Cs. Legion's sq. 565, 532 10 Pardubice, Czech Republic

[e] Department of Medical Chemistry and Biochemistry, Faculty of Medicine and Dentistry, Palacky University, Hnevotinska 3, 775 15 Olomouc, Czech Republic

Corresponding authors: *J. Storch (organic synthesis) storchj@icpf.cas.cz; **J. Vacek (electrochemistry) jan.vacek@upol.cz

Keywords

helicene • thiophene • electropolymerization • electrodeposition • carbon

---

Abstract

New materials bearing thiophene and helicene moieties were prepared by a potential-driven on/off switch strategy onto the surface of glassy carbon and indium tin oxide substrates. Specifically, a 3-([7]helicen-9-yl)-thiophene hybrid monomer was electrooxidized in acetonitrile by cyclic voltammetry with anodic potential limits of +1.5 V or +2.5 V, resulting in a conductive and non-conductive polymer, respectively. The electrochemical findings were supplemented by microscopy investigations; UV-Vis, fluorescence and vibrational spectroscopies; ^{1}H NMR spectroscopy; ellipsometry measurements and computational chemistry. The electrodeposited polymers could be used for the further development of materials applicable in organic electronics, optoelectronics and sensing technologies.

Graphical Abstract:

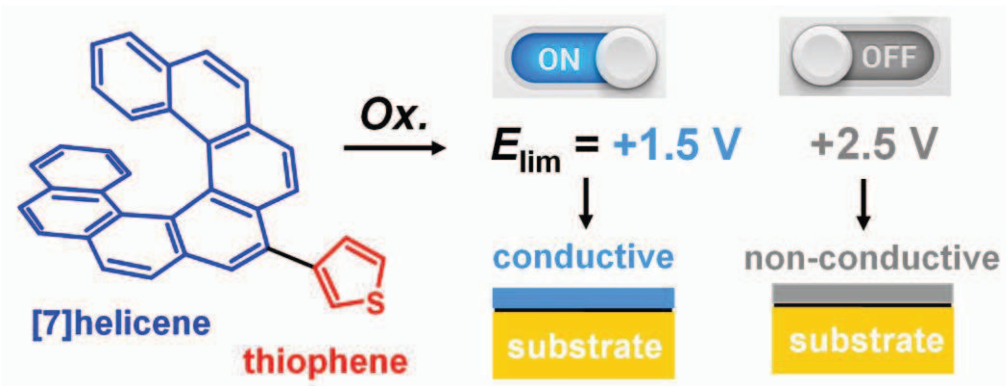

Polymers based on [7]helicene and thiophene were prepared. Conductive and non-conductive thin layers were synthesized electrochemically. Carbon and indium tin oxide substrates were used for polymer deposition. A joint experimental and computational approach was applied.

Electrochemistry has opened up the path to easy-to-handle polymer films on solid supports, applicable in electrochemical sensing, electrocatalysis, electrochromism and energy storage. We recently developed the hybrid molecule 3-([7]helicen-9-yl)-thiophene, which can be immobilized as a polymer film onto carbon and gold supports [1]. 3-([7]Helicen-9-yl)-thiophene is composed of a thiophene moiety useful for the preparation of polymeric structures applicable in organic field-effect transistors, a wide range of energy-related applications [2] and microelectronics in general [3]. Another constituent of 3-([7]helicen-9-yl)-thiophene is [7]helicene, which falls into the category of polyaromatic helical compounds called helicenes. Helicenes exhibit a non-planar topology with a C2-symmetric axis perpendicular to the axis of helicity as a result of the steric repulsive interaction between terminal aromatic rings [4]. This makes them chiral, even though they have no center of chirality. The combination of chirality and an extended π-conjugated system makes helicenes and their derivatives promising candidates for circularly polarized luminescence devices [5], novel sensing technologies [6] and chiral separation applications [7]. Moreover, linking functional molecules (like helicenes) with intrinsically conductive polymers can produce currently unexplored new materials. There have only been several examples of introducing helicene moieties into polymers to date [7].

In our previous investigation, we found that 3-([7]helicen-9-yl)-thiophene undergoes anodic reaction resulting in overoxidized layers, deposited onto surfaces of the used conductive substrates [1]. The main advantage of this procedure is that electrodeposition is quantitative process controlled by time-dependent electrochemical parameters as scan rate and number of electrochemical scans. Herein we report the electrooxidation of 3-([7]helicen-9-yl)-thiophene, resulting in conductive or non-conductive polymers based on an on/off switch mechanism in terms of the anodic potential limit applied. The formation of the polymeric films onto glassy carbon and indium tin oxide substrates was investigated using cyclic voltammetry (CV), scanning electron microscopy (SEM), atomic force microscopy (AFM), nuclear magnetic resonance (NMR) and also optical spectroscopic and computational chemistry tools.

This work deals with the formation of a [7]helicene-derived polymer material on the surface of glassy carbon (GC) and indium tin oxide (ITO) substrates using CV. The preparation of the 3-([7]helicen-9-yl)-thiophene monomer (Fig. 1A) used for electrosynthetic purposes was carried out according to a previously suggested protocol [1]. The electropolymerization of the monomer is mediated by the conjunction of extended π-conjugated [7]helicene with the electropolymerizable system of thiophene, which upon repeated anodization of the electrode (substrate) forms a polymeric structure.

CV records of the 3-([7]helicen-9-yl)-thiophene at a GCE in acetonitrile/0.1 M tetrabutylammonium perchlorate (TBAP) as the supporting electrolyte is shown in Fig. 1B. A complex multi-component anodic reaction occurs in the potential region 1-2 V *vs.* Ag/AgCl/3M KCl. During the potential cycling, a decrease in anodic currents (multi-component peak OX) is observed (Fig. 1B). This indicates the formation of the poly[3-([7]helicen-9-yl)-thiophene] film on the electrode surface, which is a barrier that hampers monomer diffusion to the anode. The above non-conductive overoxidized polymer passivating electrode surface was formed with an anodic potential limit (*i.e.* CV vertex potential) of +2.5 V (Fig. 1B). This finding is in perfect agreement with observations made under basically the same conditions with carbon fiber electrodes, where only electron tunneling at a limited rate was observed for overoxidized layers [1].

To prepare a conductive version of the poly[3-([7]helicen-9-yl)-thiophene] layer, a lower value of vertex potential needs to be applied (Fig. 1C). In this way, under cyclic anodization from 0 to +1.5 V, the formation of a conductive polymer was observed. In contrast with non-conductive poly[3-([7]helicen-9-yl)-thiophene], the conductive polymer was redox active, which is well known in the literature for polythiophene conductive polymers and their derivatives. The conductive film is characterized by a broad pair of peaks centered at *ca.* +1 V, with both the anodic and cathodic peak heights increasing proportionally to the number of CV cycles applied [8]. The formation of compact layers was confirmed using $Fe(CN)_6^{3-/4-}$ and $Ru(NH_3)_6^{3+/2+}$ redox probes according to a previously reported methodology [9]. The stability (redox activity) of the conductive version of poly[3-([7]helicen-9-yl)-thiophene] was investigated in pure supporting electrolyte under cyclic anodization from 0 to +1.2 V (Fig. 1D). After the first five CV scans, a stable CV response of the conductive polymer could be observed. The same electropolymerization and redox cycling experiments were performed using a supporting electrolyte composed of dichloromethane/0.1 M TBAP, where the resulting conductive layers were only partially stable under the experimental conditions used.

The formation of poly[3-([7]helicen-9-yl)-thiophene] structures was documented using a high-surface area carbon electrode (GC plates) by SEM (Fig. 2A-F). The results are shown for the overoxidized version of the polymer. In order to prepare a sufficiently thick layer, a low scan rate (5 mV s^{-1}) was employed, leading to a polymer approx. 4.5 µm thick after five cycles in the potential range from 0 to +2.5 V. The SEM images for the conductive polymer are qualitatively the same. The formation of poly[3-([7]helicen-9-yl)-thiophene] leads to a typical 3D structure on the substrate surface (Fig. 2A-D). When the monomer is not present in the solution, no deposit formation is observed (Fig. 2E). When the optimal conditions are not maintained, the substrate is not fully covered by the deposit. In the micrograph in Fig. 2F, the dynamics of the film formation can be easily followed, where at first local domains form, which gradually enlarge to form “isolated islands” until full coverage of the substrate surface is reached. The main factor in modulating the thickness of the deposited layers are time-dependent electrolytic parameters, which are the scan rate and number of CV scans, as previously shown [1].

In order to better characterize the poly[3-([7]helicen-9-yl)-thiophene] deposits, complementary experiments with ITO transparent electrodes were performed. CV records of the 3-([7]helicen-9-yl)-thiophene monomer are shown for both anodic potential limits leading to the non-conductive (Fig. 3A) and conductive (Fig. 3B) polymers. The electrodeposited layers are yellow and visible to the eye, as shown in the inset of Fig. 3A. Under the same experimental conditions, the voltammograms are generally very similar to that obtained at the GCE, with slight changes in the peak positions and heights. The thickness of the electrosynthesized polymers was about 50 nm based on AFM profilometric analysis. The AFM images of conductive and non-conductive poly[3-([7]helicen-9-yl)-thiophene] are shown in Fig. 3C.

To conclude the electrosynthetic results, it is important to note that thiophene alone did not lead to the polymer formation under the same conditions as for 3-([7]helicen-9-yl)-thiophene, because of the low concentration of thiophene monomer used. The minimum concentration for the electrosynthesis of conductive polythiophenes is around 10 mM [10]. Generally, the 3-([7]helicen-9-yl)-thiophene molecule undergoes electrooxidation more easily than thiophene or [7]helicene [1]. The strong involvement of the 3-([7]helicen-9-yl)-thiophene monomer in the electropolymerization process can be attributed to its electron density distribution. This is clearly documented at the HOMO level of 3-([7]helicen-9-yl)-thiophene, where the electron density is localized to the thiophene moiety (Fig. 1A). In addition, the ionization potential energy (IE) is lower for 3-([7]helicen-9-yl)-thiophene (5.552 eV) than either thiophene or [7]helicene (Fig. 1A). This result was extended by the spectroscopic investigation, where the experimental band gap (E_g) of thiophene, [7]helicene and 3-

([7]helicen-9-yl)-thiophene were estimated from the long-wavelength edge of the absorption bands (Fig. 1A) [11].

To investigate the surface chemistry of poly[3-([7]helicen-9-yl)-thiophene], Raman spectra were recorded at a wavelength of 325 nm (Fig. 4A). Both conductive and also non-conductive polymers deposited onto ITO electrodes exhibit the typical Raman characteristics observed for several carbon materials, featuring the so-called G band around 1600 cm^{-1} which is associated with sp^2 hybridized carbons and the characteristic sp^3 carbon band around 1340 cm^{-1} (D band) [9].

To determine the spectral properties of conductive and non-conductive poly[3-([7]helicen-9-yl)-thiophene] in more detail, the ITO layers were electrosynthesized from 2 mM 3-([7]helicen-9-yl)-thiophene monomer solutions. The electrodeposited layers were investigated using UV-Vis and fluorescence spectrophotometry. The UV-Vis spectra of conductive and non-conductive poly[3-([7]helicen-9-yl)-thiophene] were collected in the solid state (Fig. 5A). The strong absorbance in the region from 400-600 nm in the conductive polymer indicates a high level of conjugation compared to the non-conductive polymer. After that, dissolution experiments for both polymers were attempted using the following solvents: isopropyl alcohol, octanol, ethyl acetate, acetone, diethyl ether, octane, cyclohexane, dichloromethane and benzene, where 10 mL of solvent per ITO slide was used under mild agitation conditions, the polymer-coated ITO slide was in contact with the solvent for 24 h. Both polymers were found to only be appreciably soluble in benzene, yielding light brown solutions. The dissolution of the layer proceeds relatively slowly, which is in agreement with the polymer dissolution mechanism requiring solvent diffusion and chain disentanglement [12]. For this reason, the electrodeposited layers were dissolved in benzene using sonication procedure at the temperature of 55 °C for 3.5 h. The collected solutions were characterized using absorption and fluorescence spectroscopies, and their spectral signatures were compared to the monomeric 3-([7]helicen-9-yl)-thiophene, see inset in Fig. 5A and Fig. 5B. The benzene insoluble high-molecular fraction remains attached to the ITO substrate used for electropolymerization, which was also confirmed by UV-Vis spectrophotometry of ITO slides (not shown).

In unsubstituted oligothiophenes, the degree of oligomerization can be easily followed from the red shift of the electron transfer band, located at 243 nm for thiophene, 302 nm for bithiophene and shifting up to 432 nm in the oligomer containing five thiophene units [13]. The presence of the large delocalized π system of helicene in the 3-([7]helicen-9-yl)-thiophene monomer, oligomers and polymers results in the spectra containing broad and overlapping features, rendering quantitative estimation of the mean degree of conjugation of polymers impossible. Qualitatively, red shifts in long wavelength absorption bands indicate an increasingly higher level of conjugation in the order 3-([7]helicen-9-yl)-thiophene monomer < non-conductive oligomer < conductive oligomer < non-conductive polymer < conductive polymer. The above results are consistent with the fluorescence emission spectra, where shifts towards longer wavelengths are clearly seen for monomer, non-conductive and conductive oligomers of 3-([7]helicen-9-yl)-thiophene benzene solutions (Fig. 5B).

In addition to the above, the collected solutions were investigated using gel permeation chromatography (GPC) with UV-Vis detection at 360 nm. The oligomeric benzene-soluble fractions with molecular weights from 100 to 6000 Da (with maximum at 1500 Da) were found for both conductive and non-conductive polymeric structures using the polystyrene standard. To better characterize dissolved poly[3-([7]helicen-9-yl)-thiophene], the collected samples were also investigated using ^{1}H NMR (Fig. 6). The solution of overoxidized non-conducting polymer in benzene-d_6 does not contain helicene and thiophene signals at all. On the other hand, the spectrum of dissolved conductive poly[3-([7]helicen-9-yl)-thiophene] contains group of characteristic β-protons of thiophene ring located at 6.9-7.0

ppm [14] and signals of helicene backbone also significantly changed due to different chemical environment (Fig. 6).

Finally, the optical properties of the prepared samples were studied using ellipsometry in the infrared spectral range from 1000 to 6000 cm^{-1}. First, the ITO undercoating was characterized using a Drude-Lorentz dispersion model. The ITO coating exhibits a gradual profile of optical constants that was parametrized as an exponential decrease in the concentration of free charge carriers in the Drude oscillator. The poly[3-([7]helicen-9-yl)-thiophene] coating was analyzed using a dispersion model consisting of several Lorentz oscillators. Each oscillator exhibits particular vibrational modes in the far-infrared spectral range. The real and imaginary parts of the dielectric function are shown in Fig. 4B. The conductive and non-conductive polymers exhibit vibrational bands at about 1355, 1655 and 2930 cm^{-1}. The thickness of the coating was specified ellipsometrically to be 75 nm and 34 nm for the conductive and non-conductive polymer respectively, both of which are isotropic in nature.

Here we applied a hybrid monomer composed of [7]helicene and thiophene for the electrosynthesis of a novel polymer, poly[3-([7]helicen-9-yl)thiophene]. The potential-driven on/off switch concept was used to prepare two types of helicene-derived polymer. This concept is based on cyclic anodization of the electrode to +1.5 or +2.5 V, leading to compact conductive or non-conductive polymeric compact thin layers. The above results will serve as the basis for further applications for the preparation of helicene-based materials. The next step will be the synthesis of hybrid thiophene monomers from optically pure forms of helicene (P and M enantiomers), and finding potential applications for the further development and application of novel functional materials (*e.g.* logic networks, conductive 1/non-conductive 0), optoelectronics devices and organic electronics in general.

Experimental Section

Chemicals

Acetonitrile and dichloromethane, p.a. (Sigma-Aldrich), tetrabutylammonium perchlorate, TBAP (Fluka), potassium ferricyanide (Lachema Brno, Czech Republic), hexaammineruthenium(III) chloride (Sigma) and thiophene (Sigma) were used. 3-([7]Helicen-9-yl)-thiophene was synthesized as described in our previously published report [1]. The organic solvents used for polymer dissolution were supplied by Sigma, Merck or Lachema Brno and were p.a. grade.

Electrochemistry

Electrochemical experiments were conducted using a Nanoampere electrochemical workstation (L-Chem, CZ). A CHI MF-2012 glassy carbon electrode (disc, 3 mm in diameter), Alfa Aesar type 38021 glassy carbon plates (cut into 2 cm × 1.6 cm × 1 mm strips) and indium tin oxide (ITO)-coated glass sq slides with a surface resistivity of 8-12 Ω/sq, (Sigma Aldrich) were used as the working electrodes, Ag/AgCl/3M KCl (RE-5B, Bioanalytical Systems, Inc., IN, USA) and a platinum wire served as the reference and auxiliary electrodes, respectively. The use of an aqueous reference electrode was justified by recording the cyclic voltammogram of ferrocene [15]. The electropolymerization experiments were done from a solution of 3-([7]helicen-9-yl)-thiophene (1 mM) in acetonitrile/0.1 M tetrabutylammonium perchlorate (ACN/0.1 M TBAP) under atmospheric oxygen at 20 °C unless stated otherwise. Electrochemical data were evaluated using the software eL-ChemViewer [16].

SEM and AFM

SEM images of GC substrates were collected with JEOL JSM 7500F under the following conditions: low secondary electron image mode, beam accelerated voltage 1 kV with a resolution of 1.4 nm, magnification range from 1 000 to 40 000 times and the distance between the bottom of the objective lens and the specimen was 8 mm. The topography of the ITO samples was obtained with a Bruker Dimension Icon AFM microscope using the PeakForce mode of measurement and using soft sharp ScanAsystAir (f=70 kHz; k=0.4N/m) tips under ambient conditions.

Optical Spectroscopy Methods

Unpolarized Raman spectra were collected using a Renishaw inVia Reflex micro-Raman spectrometer with an excitation wavelength of 325 nm, operating in a standard back-scattering configuration. The Rayleigh stray light was suppressed using Edge filters. The laser beam was focused on a ~ 2 µm spot. To minimize sample degradation caused by the intense focused beam, a reduced laser power of 2.5–25 mW was applied. For ellipsometric measurements, an IR-VASE ellipsometer (J.A.Woollam) was used. UV-Vis spectra were recorded using a Cary 5000 UV-Vis-NIR spectrophotometer (Agilent, Santa Clara, USA). Fluorescence measurements were carried out in a FLS 920 fluorescence spectrometer (Edinburgh Instruments, UK) equipped with a 450 W Xe lamp and a PMT detector with a double grating monochromator. Measurements were performed with front-face geometry in quartz cuvettes. The wavelength of excitation spectra maxima was used as the excitation wavelength for fluorescence emission spectra measurement.

Dissolution of Electrodeposited Layers

ITO glasses modified by conductive or non-conductive poly[3-([7]helicen-9-yl)thiophene] layers were immersed into benzene-d_6 (2 mL) and sonicated at 55 °C for 3.5 h. The standard sonication procedure using ultrasound bath (Bandelin SONOREX 80 W) was used.

Gel Permeation Chromatography

The GPC measurements were done on a Reprosil Analytical Column using a modular system for size exclusion chromatography equipped with multiple detectors: light-scattering DAWN Helleos II (Wyatt Technologies), refraktometer Optilab t-rEX (Wyatt Technologies), light scattering detector PL ELS 1000 (Polymer Laboratories) and Chrom UVD 250 light absorption detector. The solution was filtered through 450 nm PTFE filter prior to the GPC measurement. The molar mass was recalculated to the polystyrene standard.

NMR Spectroscopy

The dissolution of poly[3-([7]helicen-9-yl)thiophene] layers were performed using benzene-*d_6*. The resulting solutions were concentrated at reduced pressure to approximately quarter-volume (*ca.* 0.5 mL) and ^{1}H NMR spectra were recorded. The ^{1}H NMR spectra were recorded using 400 MHz Bruker Advance 400 spectrometer in benzene-d_6. Chemical shifts are reported in ppm (δ) relative to TMS, referenced to signal benzene-d_6 (δ = 7.16 ppm).

Computational Details

All calculations were performed with the package Gaussian03 [17]. The structures of the studied molecules were optimized using density functional theory (DFT) with the hybrid three-parameter Becke–Lee–Yang–Parr (B3LYP) functional [18] and with the 6-311++G** basis set. Acetonitrile solvent in the DFT calculations was simulated with the polarizable continuum model (PCM). A vibrational analysis was carried out for each structure to confirm whether it corresponded to a minimum on the potential energy surface.

Acknowledgments

The authors would like to thank dr. J. Pfleger and dr. M. Netopilík (Institute of Macromolecular Chemistry of Academy of Sciences of the Czech Republic) for their technical support, especially GPC analyses. This work was financed by the Institutional Support of Palacky University in Olomouc, Czech Republic (J.V.), by the National Grid Infrastructure MetaCentrum (LM2010005, T.S.), by the Ministry of Education Youth and Sports of the Czech Republic (LO1409, J.B., LD15058, J.H., LM2015088, L.F., CEMNAT CZ.1.05/4.1.00/11.0251, M.K. and FUNBIO CZ.2.16/3.1.00/21568, L.F.), by the Technology Agency of the Czech Republic (TA04010082, J.St.), and by the Czech Science Foundation (17-02578S and 17-00089S, J.St.). The authors are indebted to Mr. Ben Watson-Jones MEng for language correction.

References

[1] J. Hrbac, J. Storch, V. Halouzka, V. Cirkva, P. Matejka and J. Vacek, *RSC Adv.* **2014**, *4*, 46102-46105.

[2] M. Zhang, X. Guo, W. Ma, H. Ade and J. Hou, *Adv. Mat.* **2014**, *26*, 5880-5885.

[3] X. Shu, Z. Li and J. Xia, *Prog. Chem.* **2015**, *27*, 385-394.

[4] M. Gingras, G. Felix and R. Peresutti, *Chem. Soc. Rev.* **2013**, *42*, 1007-1050.

[5] Y. Yang, R. C. Da Costa, M. J. Fuchter and A. J. Campbell, *Nature Photon.* **2013**, *7*, 634-638.

[6] J. Storch, J. Zadny, T. Strasak, M. Kubala, J. Sykora, M. Dusek, V. Cirkva, P. Matejka, M. Krbal and J. Vacek, *Chem. Eur. J.* **2015**, *21*, 2343 – 2347.

[7] E. Anger, H. Iida, T. Yamaguchi, K. Hayashi, D. Kumano, J. Crassous, N. Vanthuyne, C. Roussel and E. Yashima, *Polymer Chem.* **2014**, *5*, 4909-4914.

[8] M. Kabasakaloglu, T. Kiyak, H. Toprak and M. L. Aksu, *Appl. Surf. Sci.* **1999**, *152*, 115-125.

[9] R. L. McCreery, *Chem. Rev.* **2008**, *108*, 2646-2687.

[10] J. Roncali, R. Garreau, A. Yassar, P. Marque, F. Garnier and M. Lemaire, *J. Phys. Chem.* **1987**, *91*, 6706-6714.

[11] R. Schlaf, P. O. Schroeder, M. W. Nelson, B. A. Parkinson, C. D. Merritt, L. A. Crisafulli, H. Murata and Z. H. Kafafi, *Surface Sci.* **2000**, *450*, 142-152.

[12] B. A. Miller-Chou and J. L. Koenig, *Prog. Polym. Sci.* **2003**, *28*, 1223-1270.

[13] C. Van Pham, A. Burkhardt, R. Shabana, D. D. Cunningham, H. B. Mark and H. Zimmer, *Phosphorus, Sulfur, and Silicon and the Related Elements* **1989**, *46*, 153-168.

[14] a) B. Yameen, T. Puerckhauer, J. Ludwig, I. Ahmed, O. Altintas, L. Fruk, A. Colsmann and C. Barner-Kowollik, *Small* **2014**, *10*, 3091-3098; b) A. D. Mescoloto, S. H. Pulcinelli, C.

V. Santilli and V. C. Goncalves, *Polimeros* **2014**, *24*, 31-35; c) B. Krische, M. Zagorska and J. Hellberg, *Synth. Met.* **1993**, *58*, 295-307.

[15] C. Fraser and B. Bosnich, *Inorg. Chem.* **1994**, *33*, 338-346.

[16] J. Hrbac, V. Halouzka, L. Trnkova and J. Vacek, *Sensors (Switzerland)* **2014**, *14*, 13943-13954.

[17] M. J. Frisch, G. W. Trucks, H. B. Schlegel, G. E. Scuseria, M. A. Robb, J. R. Chesseman, V. G. Zakrzewski, J. A. Montgomery Jr., R. E. Stratmann, J. C. Burant, S. Dapprich, J. M. Millam, A. D. Daniels, K. N. Kudin, M. C. Strain, O. Farkas, J. Tomasi, V. Barone, M. Cossi, R. Cammi, B. Mennucci, C. Pomelli, C. Adamo, S. Clifford, J. Ochterski, G. A. Petersson, P. Y. Ayala, Q. Cui, K. Morokuma, D. K. Malick, A. D. Rabuck, K. Raghavachari, J. B. Forseman, J. Cioslowski, J. V. Ortiz, A. G. Baboul, B. B. Stefanov, G. Liu, A. Liashenko, P. Piskorz, I. Komaromi, R. Gomperts, R. L. Martin, D. J. Fox, T. Keith, M. A. AlLoham, C. Y. Peng, A. Nanayakkara, C. Gonzalez, M. Challacombe, P. M. W. Gill, B. G. Johnson, W. Chen, M. W. Wong, J. L. Andres, M. Head-Gordon, E. S. Replogle and J. A. Pople, *Gaussian 03; Gaussian Inc.: Wallingford, CT* **2003**.

[18] a) A. D. Becke, *J. Chem. Phys.* **1993**, *98*, 5648-5652; b) C. Lee, W. Yang and R. G. Parr, *Phys. Rev. B* **1988**, *37*, 785-789.

Figure legends:

Figure 1.

(A) Chemical structures of 3-([7]helicen-9-yl)thiophene, [7]helicene and thiophene with corresponding HOMO levels, band gaps (E_g) and ionization potential energies (IE). Cyclic voltammograms (**B**,**C**) of 1 mM 3-([7]helicen-9-yl)thiophene performed in acetonitrile/0.1 M TBAP at a glassy carbon electrode. CV parameters: E_{init} 0 V, vertex potentials were +2.5 (for **B**) and +1.5 (for **C**), *vs.* Ag/AgCl/3 M KCl; scan rate 100 mV s^{-1}. **(D)** Same GC electrode after electrodeposition of 3-([7]helicen-9-yl)thiophene (panel **C**) was subjected to cyclic anodization from 0 to +1.2 V in pure acetonitrile/0.1 M TBAP.

Figure 2.

SEM images of poly[3-([7]helicen-9-yl)thiophene] fully-covered surface of GC substrate (**A-D**, at different scales). Control sample of GC plate without polymer coating (**E**) and partial coverage of GC surface with polymer (**F**) are also shown. CV electropolymerization conditions were the same as in Fig. 1B, scan rate 5 mV s^{-1} (5^{th} scans).

Figure 3.

Cyclic voltammograms (**A**,**B**) of 1 mM 3-([7]helicen-9-yl)thiophene performed in acetonitrile/0.1 M TBAP at ITO electrodes. CV parameters: E_{init} 0 V, vertex potentials were +2.5 (for **A**) and +1.5 (for **B**), *vs.* Ag/AgCl/3 M KCl; scan rate 100 mV s^{-1}. Inset: ITO substrate covered with non-conductive and conductive poly[3-([7]helicen-9-yl)thiophene] structures; polymer-covered area is darker than bare unmodified electrode. **(C)** AFM images of bare, non-conductive and conductive versions of poly[3-([7]helicen-9-yl)thiophene] prepared under same conditions as in panels **A** and **B**.

Figure 4.

(A) Raman spectra of bare, non-conductive and conductive poly[3-([7]helicen-9-yl)thiophene] coated ITO slides prepared under same conditions as in Figs. **3A** and **3B**. Graph **(B)** depicts real and imaginary part of dielectric function of conductive and non-conductive polymer.

Figure 5.

(A) Normalized UV-Vis absorption spectra of non-conductive and conductive poly[3-([7]helicen-9-yl)thiophene] electrodeposited onto ITO slides. Normalized UV-Vis absorption spectra **(inset)** and fluorescence emission spectra **(B)** of 3-([7]helicen-9-yl)thiophene monomer and dissolved conductive/non-conductive polymers in benzene. The concentration of pure monomer was 200 μM (for **inset** and panel **B**). Polymers were prepared under the same conditions as in Figs. **3A** and **3B** with 3-([7]helicen-9-yl)thiophene at a concentration of 2 mM. Dissolution was performed using sonication procedure in benzene at the temperature of 55 °C for 3.5 h. For more details, see Experimental.

Figure 6.

^{1}H NMR spectra of the aromatic region (6.6-9.6 ppm) of the 3-([7]helicen-9-yl)thiophene monomer and dissolved conductive/non-conductive polymers in benzene-d_6. Dissolution was performed using sonication procedure in benzene at 55 °C for 3.5 h. For more details, see Experimental.

Figures:

Figure 1.

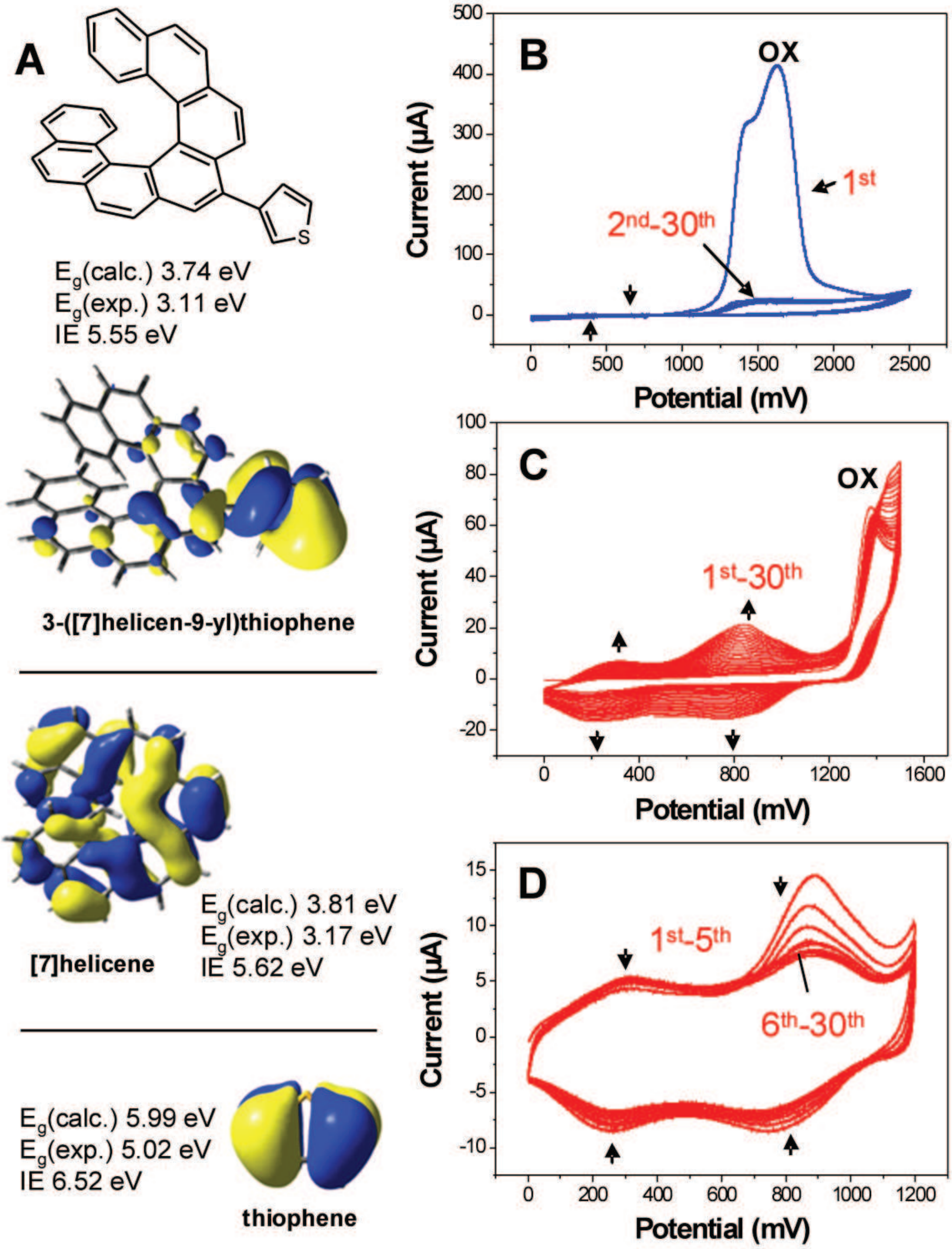

Figure 2.

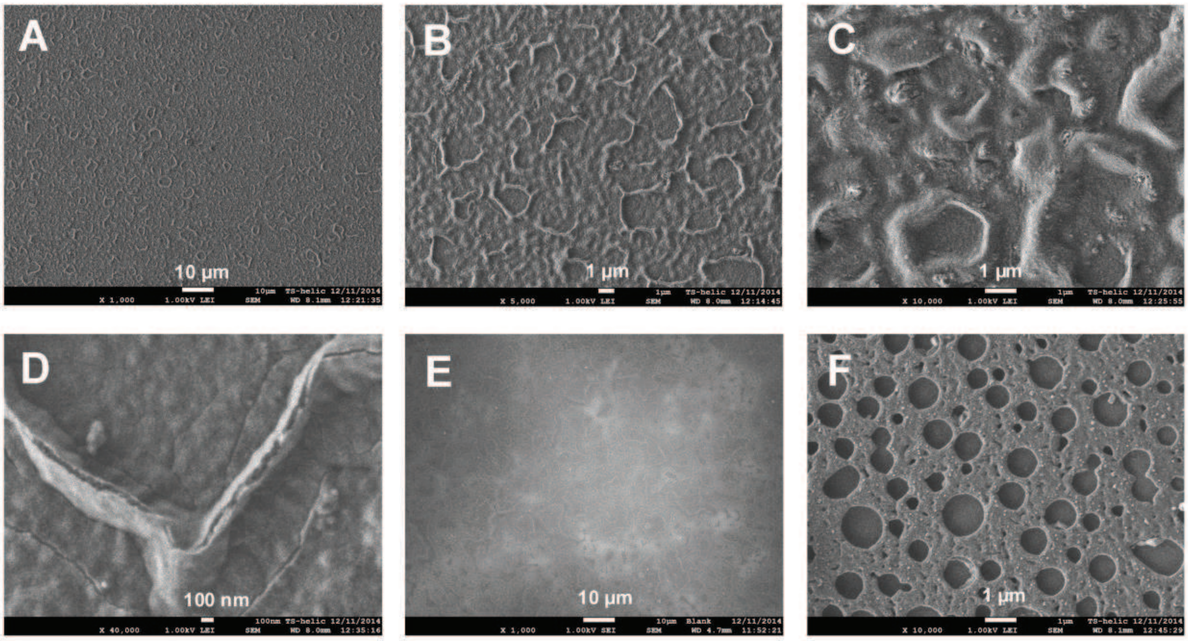

Figure 3.

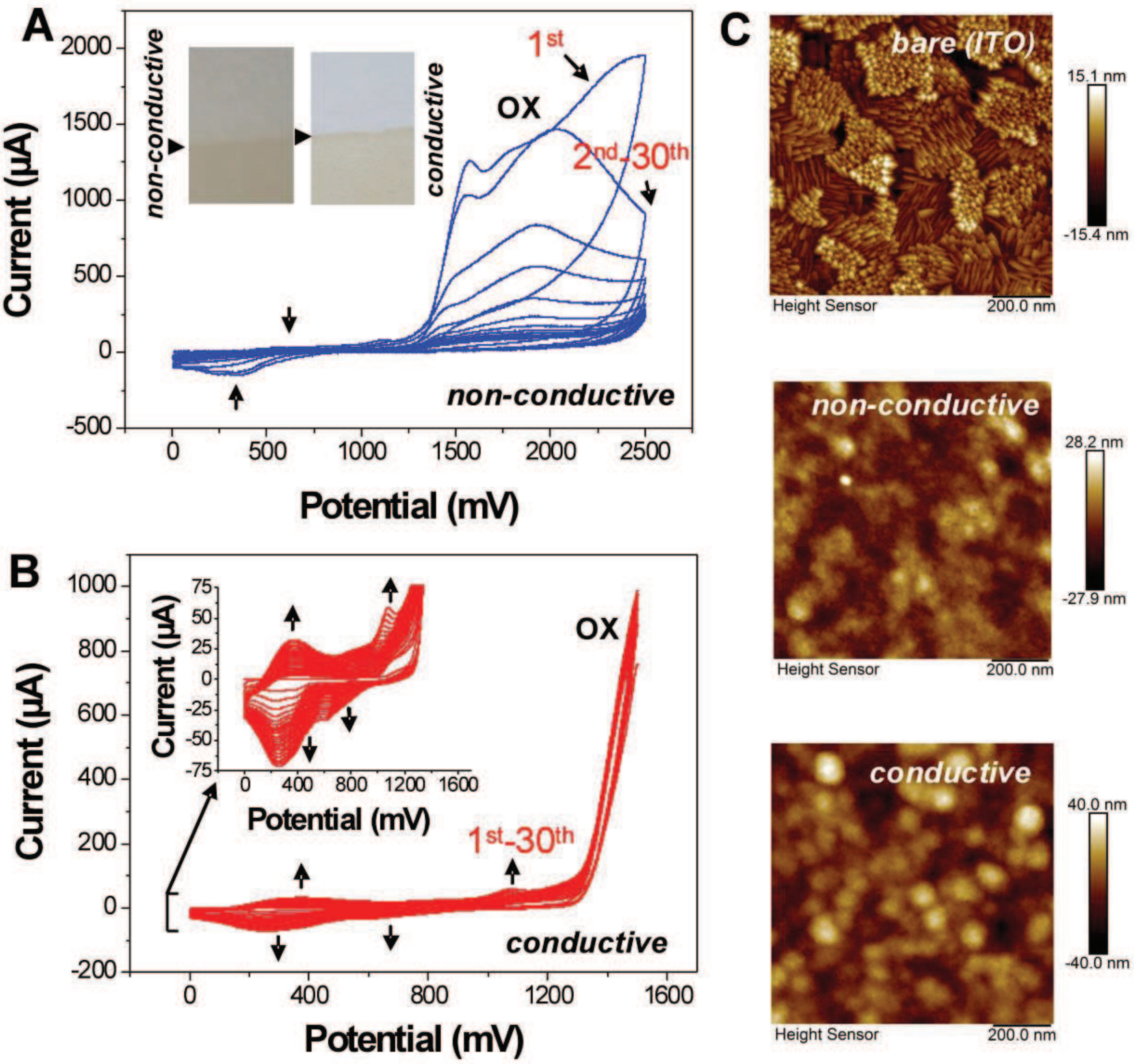
A
Current (μA)
Potential (mV)
non-conductive
conductive
1st
OX
2nd-30th
non-conductive
B
Current (μA)
Potential (mV)
OX
1st-30th
conductive
C
bare (ITO)
15.1 nm
-15.4 nm
Height Sensor
200.0 nm
non-conductive
28.2 nm
-27.9 nm
Height Sensor
200.0 nm
conductive
40.0 nm
-40.0 nm
Height Sensor
200.0 nm

Figure 4.

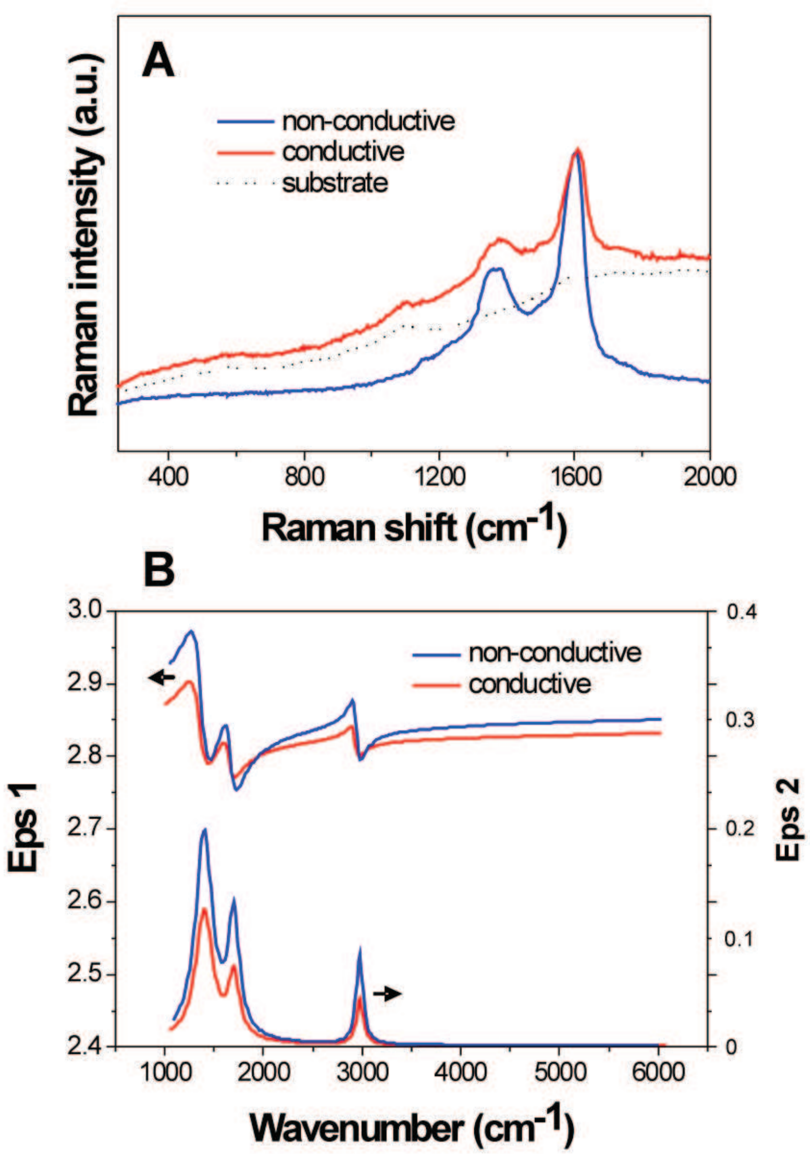
A
non-conductive
conductive
substrate
Raman intensity (a.u.)
400
800
1200
1600
2000
Raman shift (cm-1)
B
non-conductive
conductive
3.0
2.9
2.8
2.7
2.6
2.5
2.4
0.4
0.3
0.2
0.1
0
Eps 1
Eps 2
1000
2000
3000
4000
5000
6000
Wavenumber (cm-1)

Figure 5.

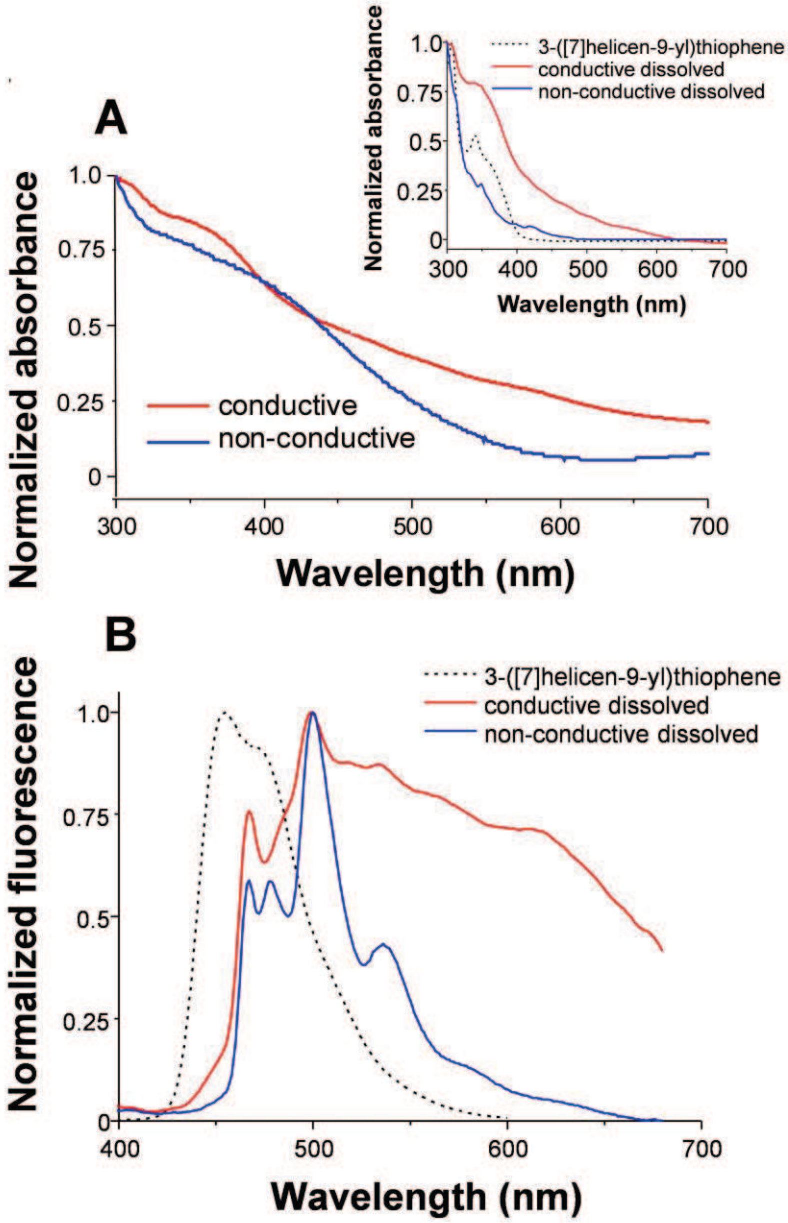

A
Normalized absorbance
1.0
0.75
0.5
0.25
0
300
400
500
600
700
Wavelength (nm)
conductive
non-conductive
Normalized absorbance
3-([7]helicen-9-yl)thiophene
conductive dissolved
non-conductive dissolved
Wavelength (nm)
B
Normalized fluorescence
3-([7]helicen-9-yl)thiophene
conductive dissolved
non-conductive dissolved
Wavelength (nm)

Figure 6.

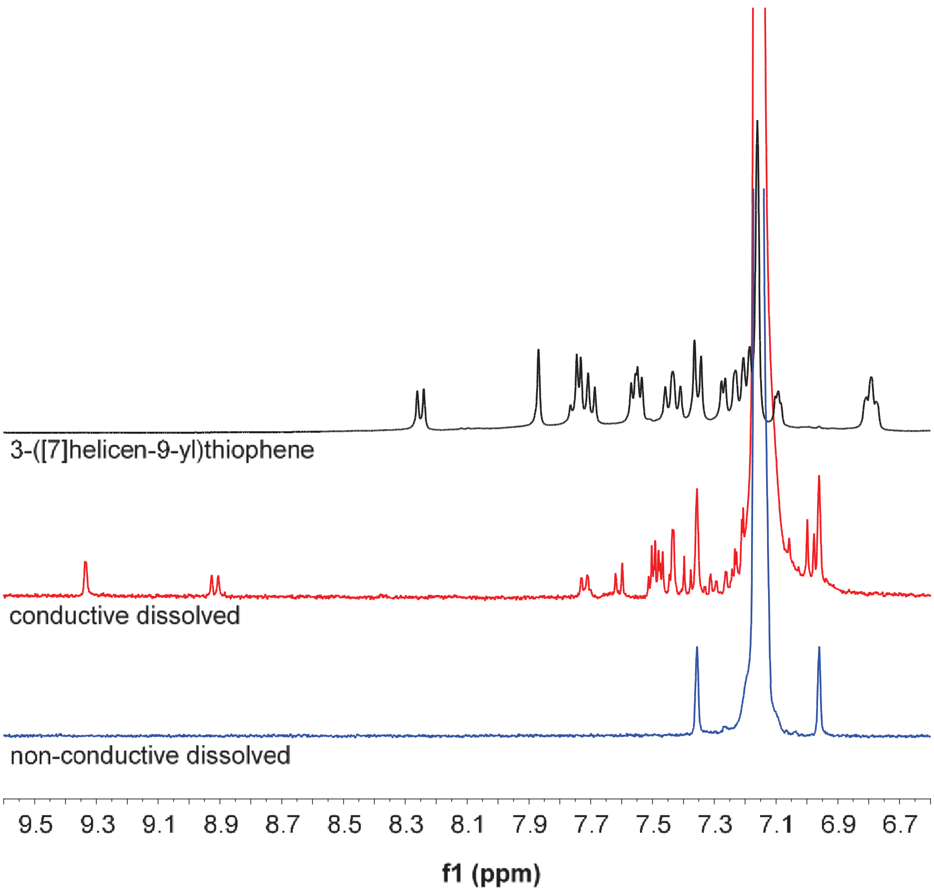
3-([7]helicen-9-yl)thiophene
conductive dissolved
non-conductive dissolved
9.5 9.3 9.1 8.9 8.7 8.5 8.3 8.1 7.9 7.7 7.5 7.3 7.1 6.9 6.7
f1 (ppm)